

②

## AD-A212 339 REPORT DOCUMENTATION PAGE

1a. REPORT SECURITY CLASSIFICATION Unclassified		1b. RESTRICTIVE MARKINGS FILE COPY	
2a. SECURITY CLASSIFICATION AUTHORITY		3. DISTRIBUTION/AVAILABILITY OF REPORT Approved for public release; distribution unlimited.	
2b. DECLASSIFICATION/DOWNGRADING SCHEDULE		5. MONITORING ORGANIZATION REPORT NUMBER(S) ARO 22644-8-MS	
4. PERFORMING ORGANIZATION REPORT NUMBER(S)		7a. NAME OF MONITORING ORGANIZATION U. S. Army Research Office	
6a. NAME OF PERFORMING ORGANIZATION Cornell University	6b. OFFICE SYMBOL (If applicable)	7b. ADDRESS (City, State, and ZIP Code) P. O. Box 12211 Research Triangle Park, NC 27709-2211	
6c. ADDRESS (City, State, and ZIP Code) Bard Hall Dept. of Materials Science & Engineering Ithaca, New York 14853-1501		9. PROCUREMENT INSTRUMENT IDENTIFICATION NUMBER DAA629-85-K-0120	
8a. NAME OF FUNDING/SPONSORING ORGANIZATION U. S. Army Research Office	8b. OFFICE SYMBOL (If applicable)	10. SOURCE OF FUNDING NUMBERS	
8c. ADDRESS (City, State, and ZIP Code) P. O. Box 12211 Research Triangle Park, NC 27709-2211		PROGRAM ELEMENT NO.	PROJECT NO.
11. TITLE (Include Security Classification) Ion Beam Analysis of Diffusion in Polymer Glasses		TASK NO.	WORK UNIT ACCESSION NO.
12. PERSONAL AUTHOR(S) Edward J. Kramer			
13a. TYPE OF REPORT Final	13b. TIME COVERED FROM 5/6/85 to 5/5/89	14. DATE OF REPORT (Year, Month, Day) 1989 August 6	15. PAGE COUNT
16. SUPPLEMENTARY NOTATION The view, opinions and/or findings contained in this report are those of the author(s) and should not be construed as an official Department of the Army position, policy, or decision, unless so designated by other documentation.			
17. COSATI CODES		18. SUBJECT TERMS (Continue on reverse if necessary and identify by block number)	
FIELD	GROUP	SUB-GROUP	
		Case II Diffusion, Rutherford Backscattering Spectrometry	
19. ABSTRACT (Continue on reverse if necessary and identify by block number)  -- SEE REVERSE --			
20. DISTRIBUTION/AVAILABILITY OF ABSTRACT <input type="checkbox"/> UNCLASSIFIED/UNLIMITED <input type="checkbox"/> SAME AS RPT. <input type="checkbox"/> DTIC USERS		21. ABSTRACT SECURITY CLASSIFICATION Unclassified	
22a. NAME OF RESPONSIBLE INDIVIDUAL		22b. TELEPHONE (Include Area Code)	22c. OFFICE SYMBOL

### Abstract

Rutherford backscattering spectrometry (RBS) and forward recoil spectrometry (FRES) have been used to the fundamentals of Case II diffusion of organic molecules (solvent) into glassy polymers. These ion beam techniques were employed to measure the velocity  $V$  of the Case II diffusion front, the diffusion coefficient  $D$  of the solvent ahead of the front and the rate of swelling  $d\phi/dt$  of the surface of the sample as well as the solvent diffusion profiles during the period before Case II diffusion has begun. A major achievement was our discovery of a simple expression for the Case II front velocity

$$V = \sqrt{\frac{D}{\phi_c} \left(\frac{d\phi}{dt}\right)_c}$$

where  $(d\phi/dt)_c$  is the swelling rate at the critical solvent volume fraction  $\phi_c$  for Case II diffusion to begin. This expression described the results quantitatively for variations in temperature, polymer plasticizer content, solvent molecular size and solvent activity, where these produced changes of up to three orders of magnitude in  $V$ . The equation can be derived from a very general version of the Thomas and Windle model for Case II diffusion; the agreement constitutes a strong test and confirmation for the general model. The original Thomas and Windle model however, made specific assumptions about the dependence of  $D$  and  $(d\phi/dt)_c$  on  $\phi$  and osmotic pressure; our experiments show that these specific assumptions are far from correct. Our results indicate that Case II diffusion results from a physico-chemically (osmotic pressure) driven yielding of the polymer glass analogous to the familiar mechanical yielding; the almost discontinuous increase in diffusion coefficient that accompanies the yielding accounts for the formation of the front.

# Ion Beam Analysis of Diffusion in Polymer Glasses

Edward J. Kramer

August 1989

U. S. Army Research Office

Contract/Grant Number DAAG29-85-K-0120

Department of Materials Science and Engineering

Cornell University

Ithaca, NY 14853

APPROVED FOR PUBLIC RELEASE:

DISTRIBUTION UNLIMITED

THE VIEWS, OPINIONS AND/OR FINDINGS CONTAINED IN THIS REPORT  
ARE THOSE OF THE AUTHOR AND SHOULD NOT BE CONSTRUED AS  
OFFICIAL DEPARTMENT OF THE ARMY POSITION, POLICY OR DECISION,  
UNLESS SO DESIGNATED BY OTHER DOCUMENTATION

## Abstract

Rutherford backscattering spectrometry (RBS) and forward recoil spectrometry (FRES) have been used to study the fundamentals of Case II diffusion of organic molecules (solvent) into glassy polymers. These ion beam techniques were employed to measure the velocity  $V$  of the Case II diffusion front, the diffusion coefficient  $D$  of the solvent ahead of the front and the rate of swelling  $d\phi/dt$  of the surface of the sample as well as the solvent diffusion profiles during the period before Case II diffusion has begun. A major achievement was our discovery of a simple expression for the Case II front velocity

$$V = \sqrt{\frac{D}{\phi_c} \left(\frac{d\phi}{dt}\right)_c}$$

where  $(d\phi/dt)_c$  is the swelling rate at the critical solvent volume fraction  $\phi_c$  for Case II diffusion to begin. This expression described the results quantitatively for variations in temperature, polymer plasticizer content, solvent molecular size and solvent activity, where these produced changes of up to three orders of magnitude in  $V$ . The equation can be derived from a very general version of the Thomas and Windle model for Case II diffusion; the agreement constitutes a strong test and confirmation for the general model. The original Thomas and Windle model however, made specific assumptions about the dependence of  $D$  and  $(d\phi/dt)_c$  on  $\phi$  and osmotic pressure; our experiments show that these specific assumptions are far from correct. Our results indicate that Case II diffusion results from a physico-chemically (osmotic pressure) driven yielding of the polymer glass analogous to the familiar mechanical yielding; the almost discontinuous increase in diffusion coefficient that accompanies the yielding accounts for the formation of the front.

on For

CA&I

SA&I

Used

Station

By _____	
Distribution/	
Availability Codes	
Dist	Avail and/or Special
A-1	



Two ion beam analysis techniques, Rutherford backscattering spectrometry (RBS) and forward recoil spectrometry (FRES) were used to measure the volume fraction  $\phi$  versus depth  $x$  profiles for various organic molecules diffusing into polystyrene (PS). Experiments were carried out using *n*-iodoalkanes where the iodine nucleus was a convenient tag for RBS and using *d*-toluene where the deuterium nucleus could be profiled using FRES. Samples in the form of PS films  $\sim 10\mu\text{m}$  thick were cast on aluminum substrates. These films were exposed to various activities of solvent vapor by placing them in flasks, each containing a reservoir of PS granules impregnated with the appropriate amount of solvent. The flasks were suspended in a constant temperature water bath. After various times of exposure, films were removed and immediately quenched into liquid nitrogen to arrest the diffusion of solvent. The samples were then affixed to a copper block under liquid nitrogen and transferred via a dry nitrogen gas filled glove bag to the liquid nitrogen cooled stage of the ion beam analysis chamber.

Early in the experiments it was found that for certain solvents, the details of the sample arrangement in the exposure flask affected the results. It was determined that these effects were due to both convective mass transfer limitations across the gaseous boundary layer adjacent to the sample and to exhaustion of solvent vapor from the convection cell above the bottom of the sample. The effects were worst for low vapor pressure solvents under rapid sorption conditions. A general criterion was developed to predict when solvent absorption is likely to be limited by vapor phase transport or exhaustion effects [1]. To minimize these effects it was found important to:

1. Use samples which have only a small area of polymer film; in subsequent experiments samples with  $0.2 \text{ cm}^2$  area were used.

2. Place the samples as close to the bottom (reservoir) of the flask as possible; our samples were placed 1 cm above the reservoir.

3. Expose only one sample at a time as the boundary layers between two samples can significantly interfere.

4. Move the sample in the flask if possible to stimulate forced convection. Practically we used such motion experiments to ensure that our exposure conditions were not in a regime where vapor transport limitations were important. All results reported here were obtained under conditions where vapor transport limitations were not important.

At high enough activities of vapor in the reservoir, Case II diffusion was observed for all iodoalkanes and d-toluene. Previous workers have given various criteria for Case II diffusion, e.g. linear weight gain with time, the appearance of an optically anisotropic swollen layer at the sample surface which moves into the sample at a constant velocity or simply the inability to fit the diffusion data with Fickian formulae. With our microscopic depth profiling capability we can be more specific. Case II diffusion initially (at small exposure times) appears to be nothing out of the ordinary. Figure 1 shows four different depth profiles for iodohexane diffusing into PS from a reservoir with an equilibrium activity  $a_e = 0.37$  corresponding to a volume fraction  $\phi$  of solvent of 0.16 at  $30^\circ \text{C}$ . Note that after the first two exposure times, 10,000 and 60,000 seconds, the volume fraction profiles appear rather Fickian, with one exception. The volume fraction of the iodohexane at the surface does not come to local equilibrium with the reservoir ( $\phi_e = 0.16$ ) but instead grows slowly toward that

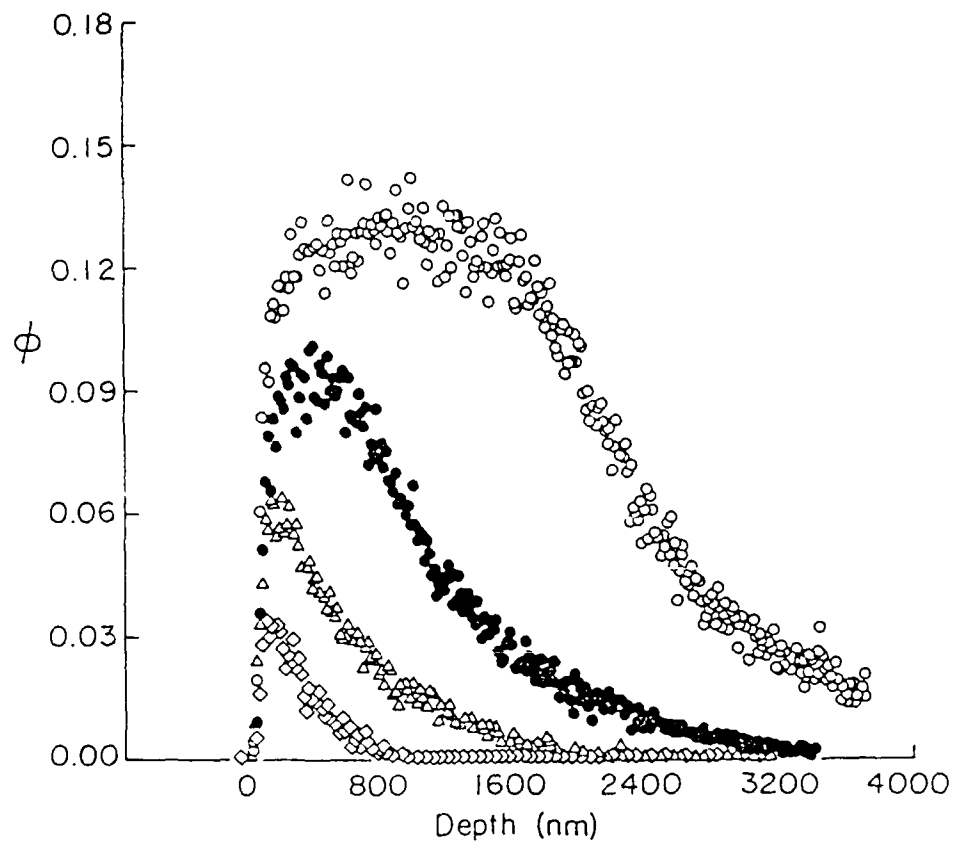


**Figure 1** A family of volume fraction versus depth profiles of iodohexane in polystyrene at  $a_e=0.37$  ( $\phi_e=0.16$ ),  $T=30^\circ\text{C}$  after exposure times  $t=3.3 \times 10^5$  ( $\circ$ ),  $1.6 \times 10^5$  ( $\bullet$ ),  $6 \times 10^4$  ( $\Delta$ ) and  $10^4$  ( $\square$ ) seconds.

equilibrium value as the exposure time increases. For the latter two exposure times, 160,000 and 330,000 seconds, however a "front" has formed and the diffusion behind that front is rapid enough that there is a negligible gradient in volume fraction there. This front, once formed, moves into the sample at a constant velocity, accounting for the linear weight gain kinetics often observed for Case II diffusion. The time that it takes to form the front has been also observed in weight gain studies and is often called the induction time. We find for the entire series of iodoalkanes that Case II diffusion begins, i.e. the front forms, when the volume fraction of solvent at the surface exceeds a certain critical volume fraction of approximately 0.12 at  $a_e = 0.45$ . If the equilibrium volume fraction  $\phi_e$  is less than this value, Case II diffusion is never observed, regardless of how long we expose the sample. All that happens is a slow increase in the surface volume fraction toward the equilibrium value and an approximately Fickian diffusion of solvent from that time-varying surface volume fraction into the sample.

One should note that the slow increase in surface volume fraction toward equilibrium does not stop at the critical concentration for Case II diffusion to begin but continues with no apparent discontinuity in rate. We can measure the kinetics of this surface swelling using the ion beam analysis techniques; such measurements were simply not possible with the cruder techniques available to earlier experimenters. As an example we show in Figure 2 measurements of the surface volume fraction  $\phi_s$  of iodopentane as a function of PS exposure time to a reservoir with  $a_e = 0.45$ . These data will be important later in testing various models of Case II diffusion.

$$d_e = 0.45$$

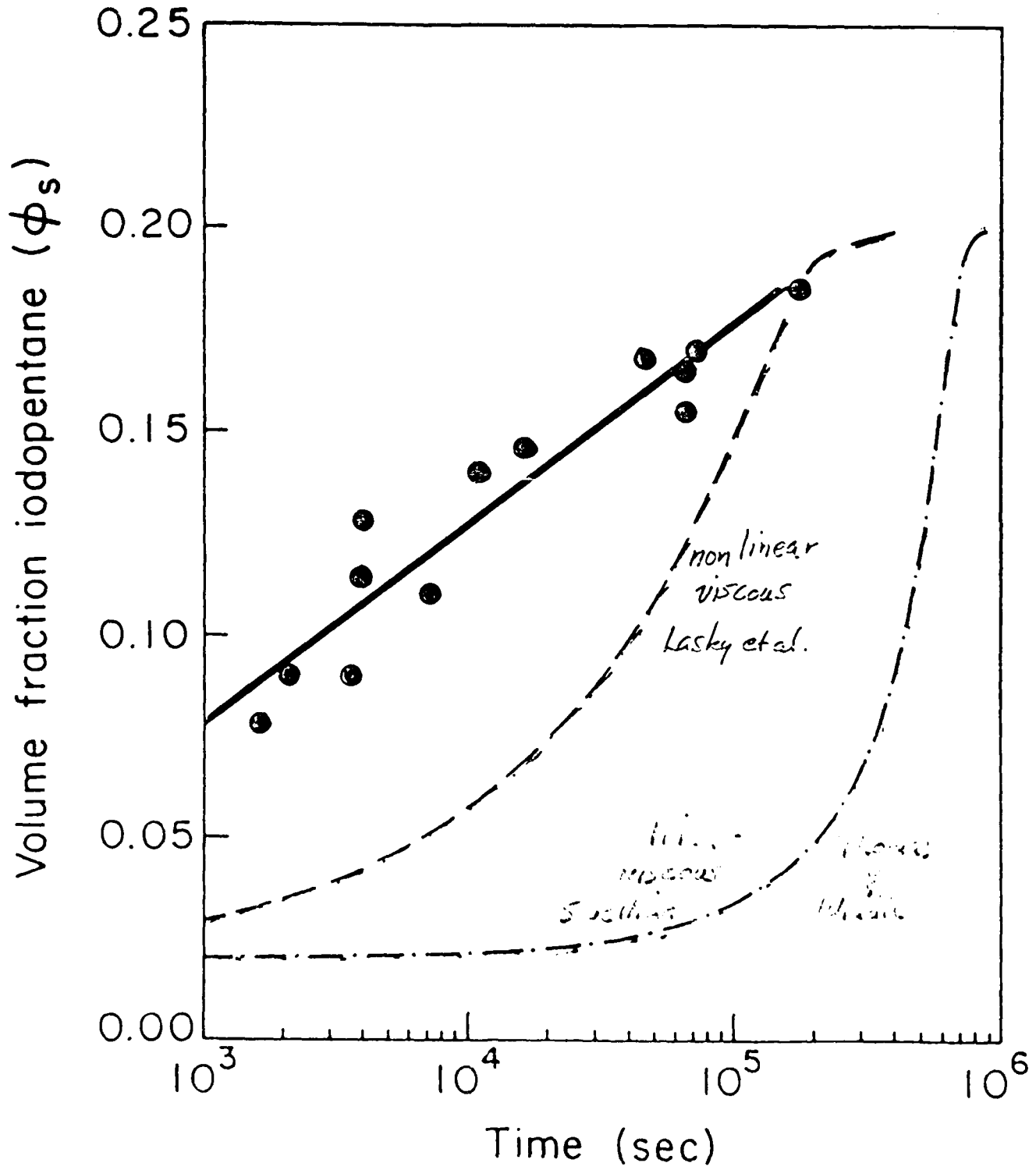


Figure 2

Once we understood the nature of the initial induction time we were able to devise other methods for measuring the surface volume fraction during this interval. In particular we developed a quartz crystal microbalance technique [2] by which the mass gain of a glassy PS thin film could be measured continuously as it was exposed to the solvent reservoir. As long as the surface volume fraction is below the critical value we were able to extract the surface volume fraction from the data using a Laplace transform method; the values so extracted were shown to be in good agreement with those directly measured from RBS under the same conditions.

Using the ion beam analysis techniques we were able to measure yet another crucial characteristic of Case II diffusion that had escaped the lower resolution methods of earlier workers, namely the diffusion profile ahead of the front. We found that the diffusion there was well described by the Fickian diffusion ahead of a moving boundary, i.e.

$$\phi(x) = \phi_c \exp\left(-\frac{Vx}{D}\right) \quad (1)$$

where  $x$  is the distance ahead of the boundary,  $V$  is the velocity of the boundary (easily measured by RBS) and  $D$  is a constant diffusion coefficient in the glass ahead of the boundary. By fitting a simulation of the RBS spectrum using this solution to the measured spectrum, we were able to extract the value of the diffusion coefficient [3]. An example of the fit, and its sensitivity to  $D$ , is shown in Figure 3. We found that these values of  $D$ , measured from the diffusion ahead of the Case II front, were in good agreement with values of  $D$  extracted from the volume fraction profiles measured during the induction time, i.e. before Case II diffusion began [4].

We were also able to measure the exchange diffusion coefficient  $D^+$

iodoheptane in PS ( $d_e = 0.45$ ) 191100 s

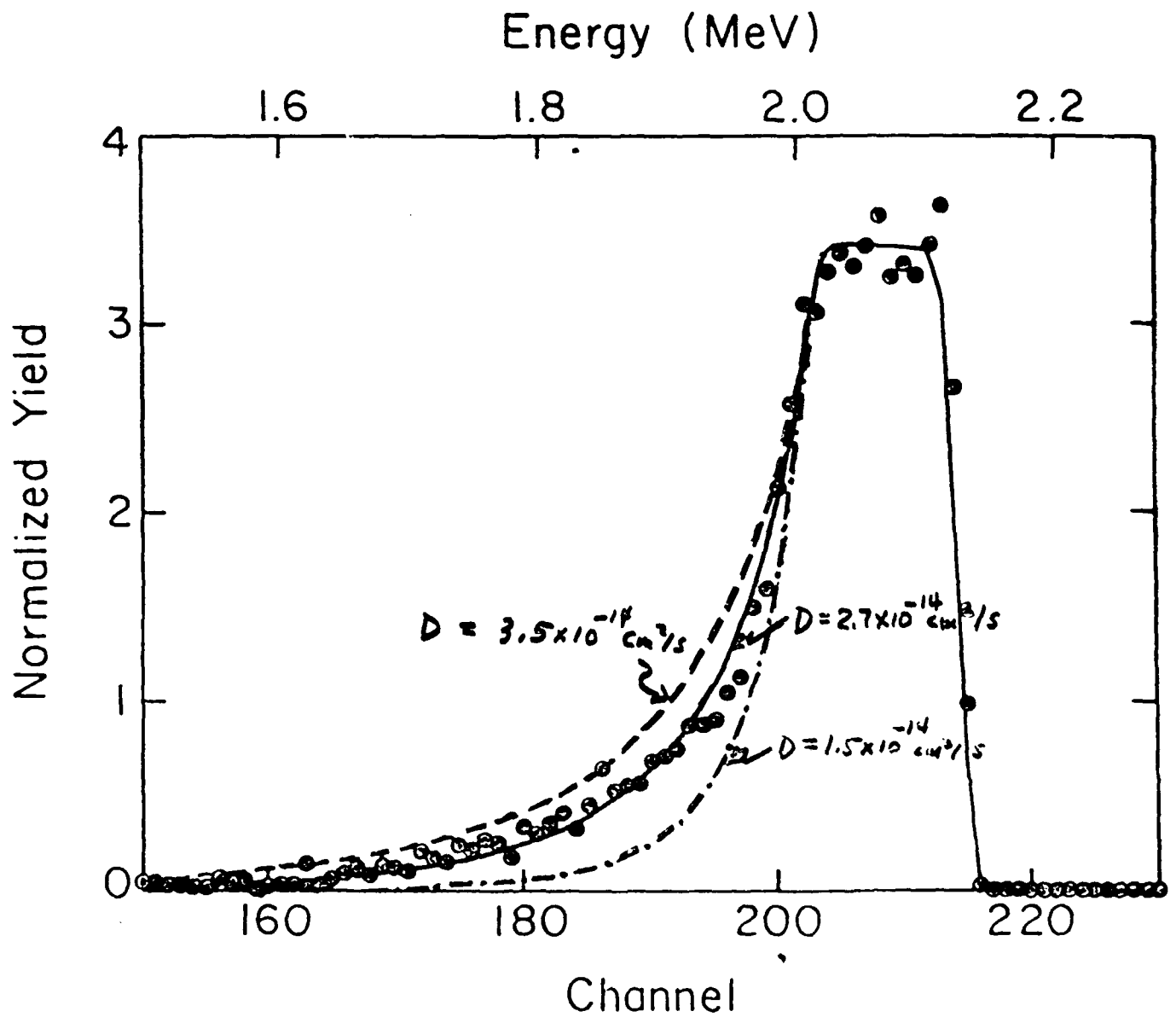


Figure 3

for d-toluene using FRES. In these experiments the PS was preswollen with protonated toluene to the same equilibrium volume fraction as the reservoir eventually used for the d-toluene exposure. In these experiments, toluene diffuses out and d-toluene diffuses in so that there is no net swelling of the PS. The exchange diffusion coefficient so measured for d-toluene in PS was in good agreement with  $D$  measured from the diffusion profile ahead of the Case II front (where the PS certainly swells simultaneously) and also with  $D$  measured from the concentration profiles corresponding to reservoir volume fractions below the critical value for Case II diffusion to begin. These results show that the value of the solvent diffusion coefficient in the glass is approximately independent of the volume fraction of solvent up to the critical volume fraction  $\phi_c$  and that its value is not sensitive to whether the PS is swelling or not.

To reinforce the idea that the  $D$ 's extracted from the diffusion profile ahead of the Case II front are the correct diffusion coefficients in the glass, we plot in Figure 4 the diffusion coefficients measured for the iodoalkanes and d-toluene versus their average molecular diameters. Also plotted in this Figure are data from spherical and non-spherical molecules diffusing at very low concentrations into PS at room temperature from the work of Berens. The magnitudes of our diffusion coefficients are in excellent agreement with those of similar non-spherical molecules measured by an entirely different technique. The diffusion coefficients of the iodoalkanes decrease markedly with molecular size, with iodopropane having the largest ( $\sim 6 \times 10^{-12} \text{cm}^2/\text{s}$ ) and iodooctane, the lowest ( $\sim 3 \times 10^{-15} \text{cm}^2/\text{s}$ ).

The final parameter that we can measure readily using the ion beam analysis techniques is the Case II front velocity  $V$  from plots of the

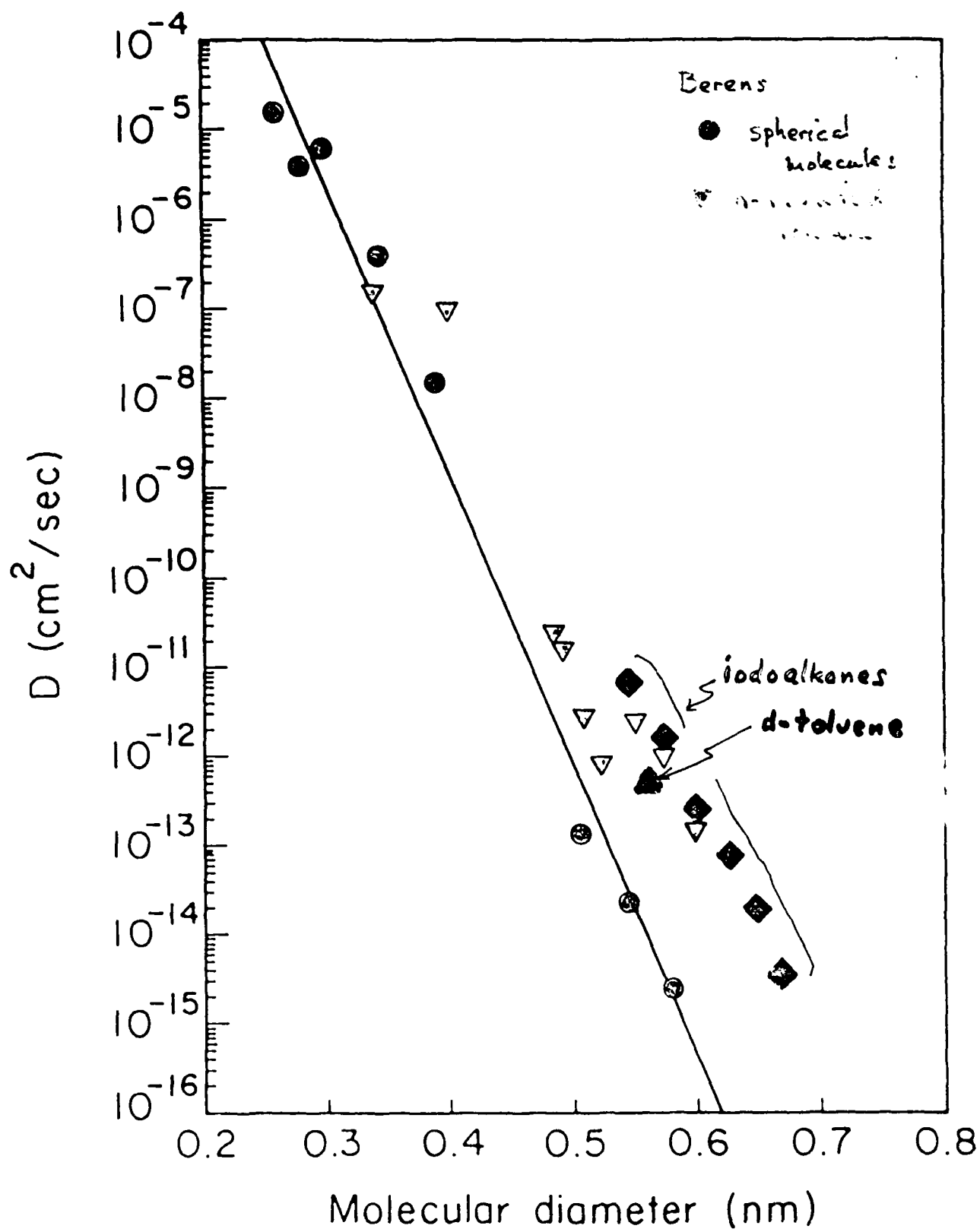
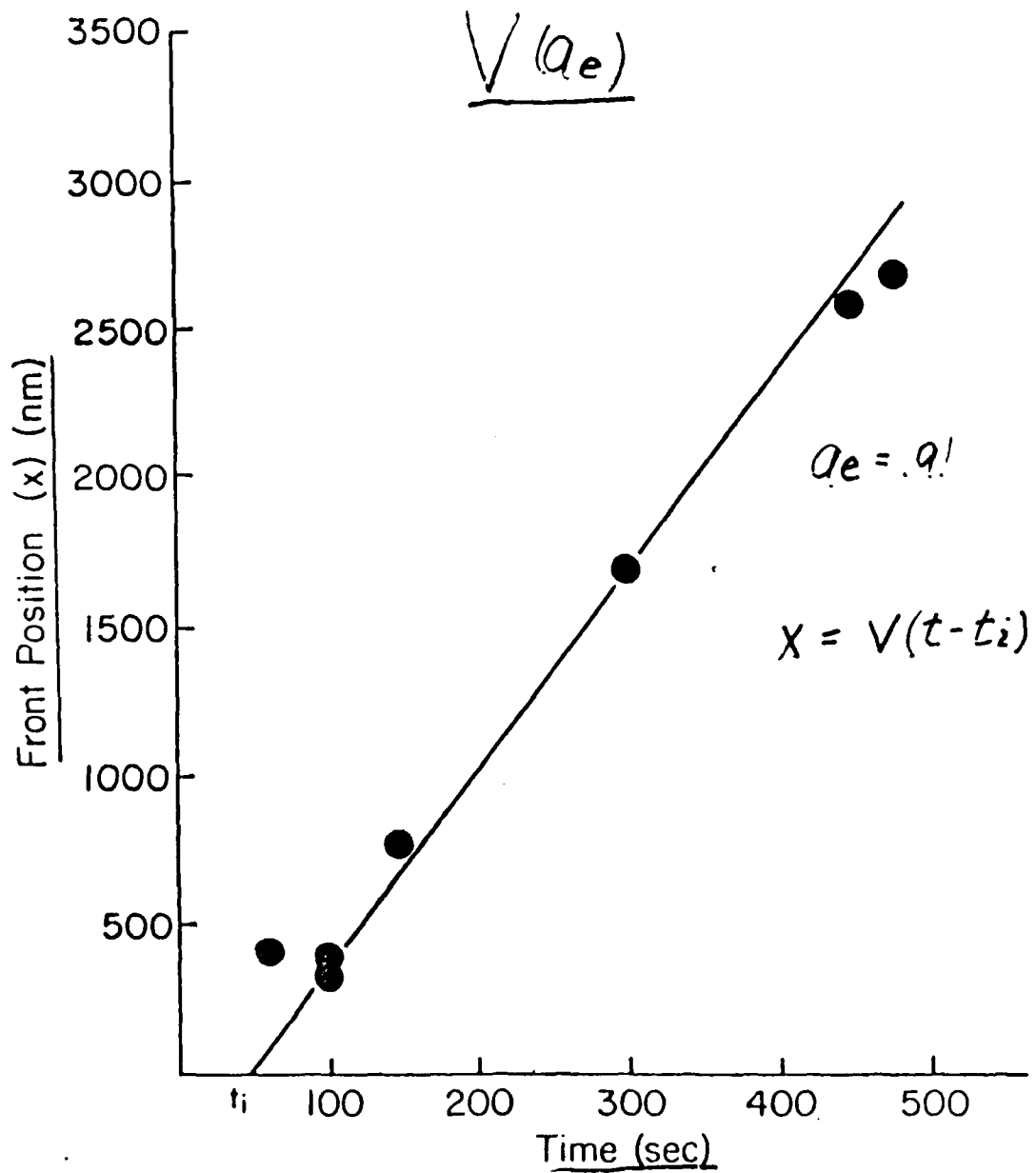


Figure 4

front depth versus time like that shown in Figure 5. The front velocity is the most important parameter of Case II diffusion in that it is dominant in determining the solvent uptake of the sample. What has been mysterious is the extreme sensitivity of the Case II velocity to the variables of the diffusion experiment; it increases orders of magnitude with small increases in temperature, activity of the solvent, size of the solvent and plasticizer content. An example is shown in Figure 6 where the front velocity is shown as a function of solvent activity. Since we have shown that the diffusion coefficient of the solvent in the glass is insensitive to solvent activity, the marked increase in  $V$  observed must be due primarily to other causes. The question of what controls, and how to predict, the front velocity was the most important question in the area of Case II diffusion. The resolution of this question is the major achievement of our AROD sponsored project.

We began our search for answers with what seemed to us to be the most physically reasonable model of Case II diffusion, that put forward in the early part of this decade by Thomas and Windle. Thomas and Windle treated the problem as a coupled deformation and diffusion problem. They reasoned that the glassy nature of the polymer would cause it to resist swelling rapidly to accept the equilibrium amount of solvent; such swelling would occur only slowly as the polymer glass relaxed toward a new equilibrium configuration which allowed for the substantial sorption of solvent. They recognized that the driving force for this relaxation was the osmotic pressure of the solvent which is given by

$$P_{os} = \frac{k_B T}{\Omega} \ln\left(\frac{a_e}{a}\right) \quad (2)$$



**Figure 5** The Case II front position versus time for iodo-hexane in polystyrene at  $a_e=0.91$  and  $T=25^{\circ}\text{C}$ . The slope is the front velocity (6.7nm/s) and  $t_i$  is the induction time which is 48 seconds.

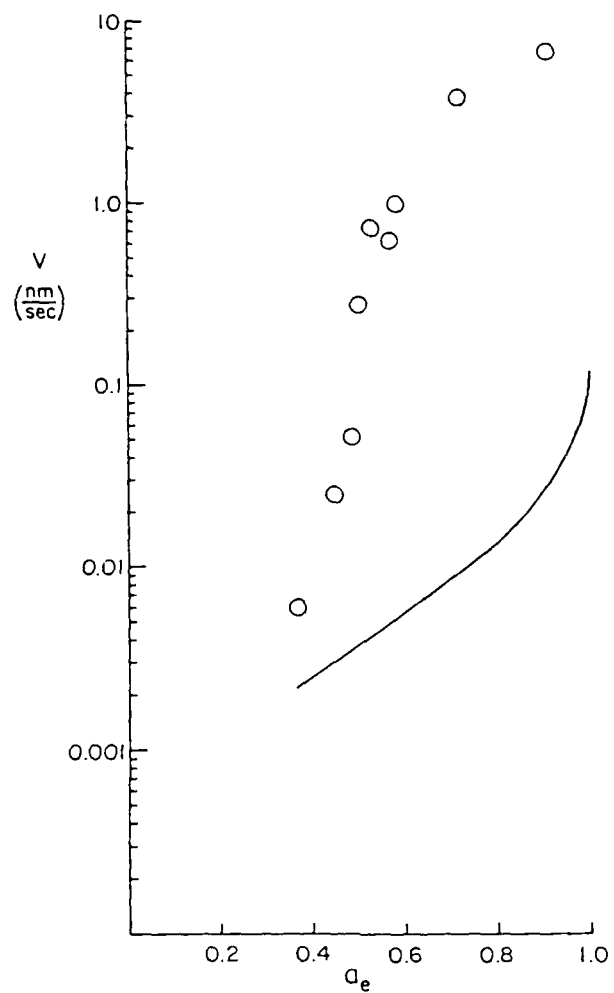


**Figure 6** The Case II front velocity versus penetrant activity for iodohexane in polystyrene at  $T=25^{\circ}\text{C}$ .

where  $a$  and  $a_e$  are the actual and equilibrium activities of the solvent and  $\Omega$  is the partial molecular volume of the solvent. The swelling rate is driven by the osmotic pressure in a manner analogous to the way the mechanical strain rate of the glass is driven by a mechanical stress. For diffusion perpendicular to the broad face of a smooth sample, the osmotic stress state is uniaxial and normal to the surface, due to the constraint of the underlying, unswollen polymer glass. This stress eventually produces the uniaxially oriented polymer behind the front. The relation between swelling rate and strain rate can be written in a very general way as [5]

$$\frac{\partial \phi}{\partial t} = g(P_{os}, \phi) \quad (3)$$

where  $g$  is some function of  $P_{os}$  and  $\phi$ .

Thomas and Windle assumed that this relation was linear viscous, i.e., that the swelling rate is proportional to  $P_{os}$ , with a "viscosity"  $\eta$  that decreases exponentially with  $\phi$  to account for the effect of plasticization. From our measurements of the swelling kinetics we were able to test their assumption [6]; not surprisingly the predictions of this simple form of the function  $g$  are far from accurate. An example can be seen in Figure 2 where the dot-dashed curve represents the best fit of the data to the linear viscous function. We tried initially to improve this fit by incorporating the nonlinear stress dependence observed for tensile creep of PS at low stresses [7]; while this produced a reasonable fit at very low vapor activities it still falls well short of an adequate description at higher activities as can be seen by comparing the dashed curve with the data in Figure 2. It is therefore best to regard  $g$  in Eq. 3 as a function to be determined

empirically.

Thomas and Windle then wrote down the diffusion equation in the form:

$$\frac{\partial \phi}{\partial t} = \frac{\partial}{\partial x} \left\{ D(\phi) \left[ \frac{\partial \phi}{\partial x} + \frac{\Omega \phi}{k_B T} \frac{\partial P_{os}}{\partial x} \right] \right\} \quad (4)$$

where the first term in brackets is the usual Fickian term whereas the second is a "drift" term due to the gradient in osmotic pressure. They assumed that  $D(\phi)$  was an exponentially increasing function of  $\phi$  (Remember we found experimentally that  $D$  does not vary markedly with  $\phi$  until the critical  $\phi$  is reached whereupon it increases discontinuously by at least several orders of magnitude.) and solved the coupled differential equations, Eqs. 3 and 4, numerically to obtain the concentration versus depth profiles after various time steps. We realized that if Eq. 3 was inverted to give  $P_{os}$  as a function of  $\partial \phi / \partial t$ , this could be substituted into Eq. 4 to give a single uncoupled, but nonlinear, partial differential equation which could be investigated in much more depth than Thomas and Windle's few numerical profiles [8]. After proving that, if the increase in  $D$  at  $\phi_c$  is large, this equation does have a steady state solution corresponding to a front moving at a constant velocity  $V$  allowing us to write

$$\frac{\partial \phi}{\partial t} = -V \frac{\partial \phi}{\partial x} \quad (5)$$

and thus to transform Eq. 4 into an ordinary differential equation, we studied the properties of the solution in more detail. It is easy to prove that

the osmotic pressure always has a maximum just ahead of the front; at the maximum, and it turns out in fact even well away from the maximum for the experimentally weak dependence of  $P_{os}$  on  $\partial\phi/\partial t$ , the drift term in Eq. 4 is negligible, so that the governing differential equation for diffusion is just

$$V \frac{\partial\phi}{\partial x} = - \frac{\partial}{\partial x} \left\{ D(x) \frac{\partial\phi}{\partial x} \right\} \quad (6)$$

which has as its solution the exponentially decreasing diffusion profile of Eq. 1 if  $D(x)$  is  $D$ , a constant, in agreement with experiment. Moreover since from Eq. 1

$$\frac{\partial\phi}{\partial x} = - \frac{V\phi}{D} \quad (7)$$

we can solve Eq. 5 for  $V$ , viz:

$$V = \sqrt{\frac{D}{\phi_c} \left. \frac{d\phi}{dt} \right|_c} \quad (8)$$

where all the quantities inside the square root are to be evaluated at the critical volume fraction for Case II diffusion to begin (which is close to the maximum in the osmotic pressure). Equation 8 thus offers us a chance to predict quantitatively the Case II front velocity; however since simple models do not suffice to predict the swelling rate at the critical volume fraction,  $d\phi/dt |_c$  it will have to be measured.

We have tested the validity of Eq. 8 in a number of ways. In one test the temperature dependence of  $V$ ,  $D$  and  $d\phi/dt |_c$  were measured for

iodohexane diffusion into PS using RBS [9]. All three quantities were thermally activated with activation enthalpies of 1.07 eV, 0.60 eV and 1.76 eV respectively. Since  $\phi_c$  is approximately constant, we can use the latter two values with Eq. 8 to predict the activation enthalpy for the velocity; the result, 1.18 eV, is in reasonable agreement with the measured value of 1.07 eV. A similar test was carried out for d-toluene diffusing into PS with similarly good agreement between Eq. 8 and experiment [10].

We have also compared the magnitude of the  $V$  predicted from Eq. 8 using the experimentally measured values of  $D$  and  $d\phi/dt|_c$ , with the measured  $V$ . Figure 7 shows the measured and predicted  $V$ 's for iodo-hexane diffusion in PS that was plasticized with various amounts of 1) dioctylphthalate and 2) with a low molecular weight PS oligomer ( $M_w = 600$ ). The agreement between the predicted and measured velocities is excellent. Figure 8 shows a similar plot of the measured and predicted  $V$ 's for the series of iodoalkanes diffusing into PS. Again the agreement is excellent. These tests, as well as less extensive comparisons for different activities of iodo-hexane, show conclusively that the simple square root relation of Eq. 8 can be used to accurately predict the Case II front velocity. It also provides important evidence that the basic physical picture behind the Thomas and Windle model of Case II diffusion is correct.

The discrepancies between the prediction of the Thomas and Windle model and experiment lie in the unrealistic assumption it makes about the law governing the swelling rate, i.e. the linear viscous assumption for the function  $g$  which supposes that  $g$  is linear in  $P_{OS}$ . How far this assumption is from being true can be illustrated by the following. Ron Lasky [3,4] showed by exposing polystyrene to different activities of iodo-hexane that the

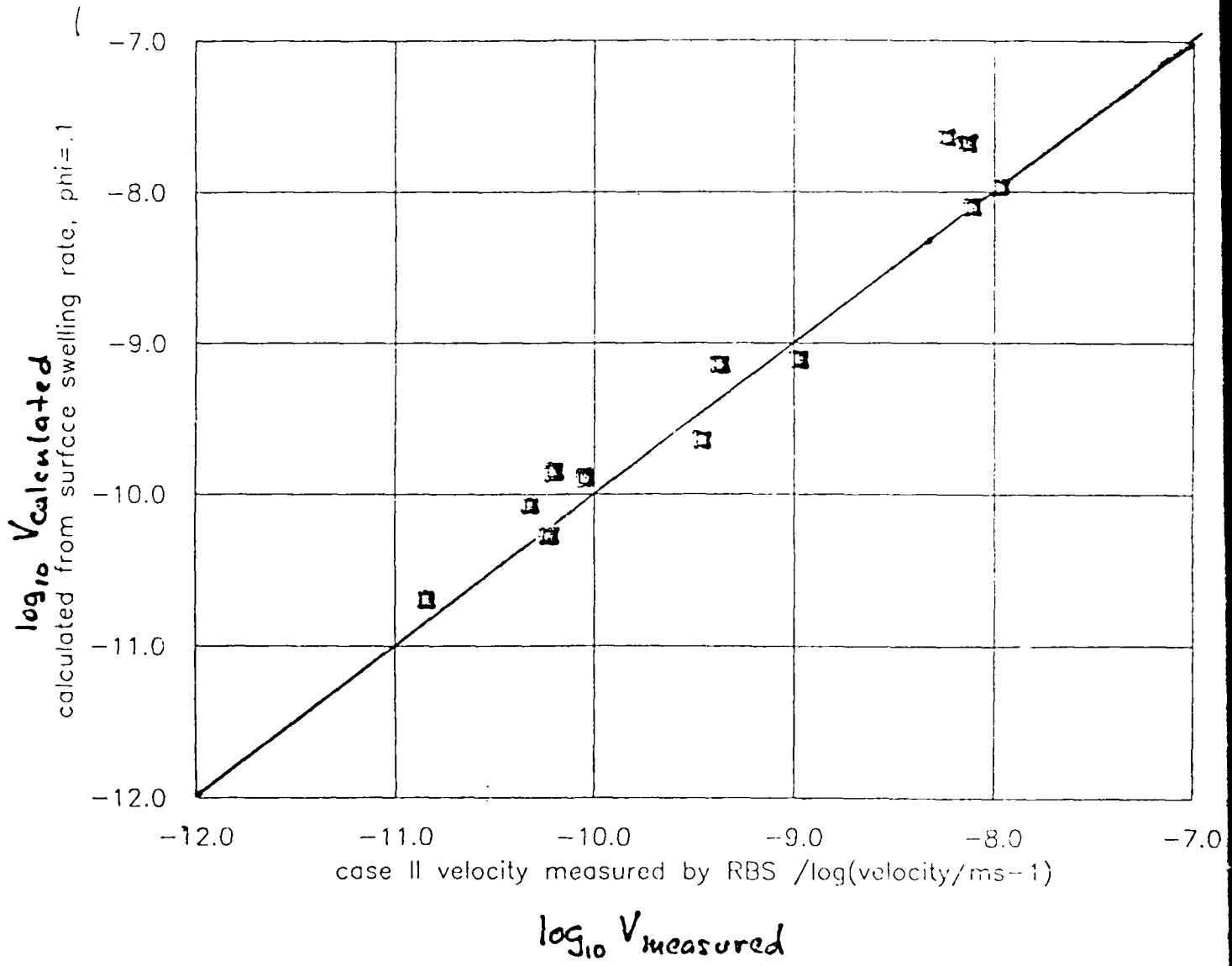


Fig. 7

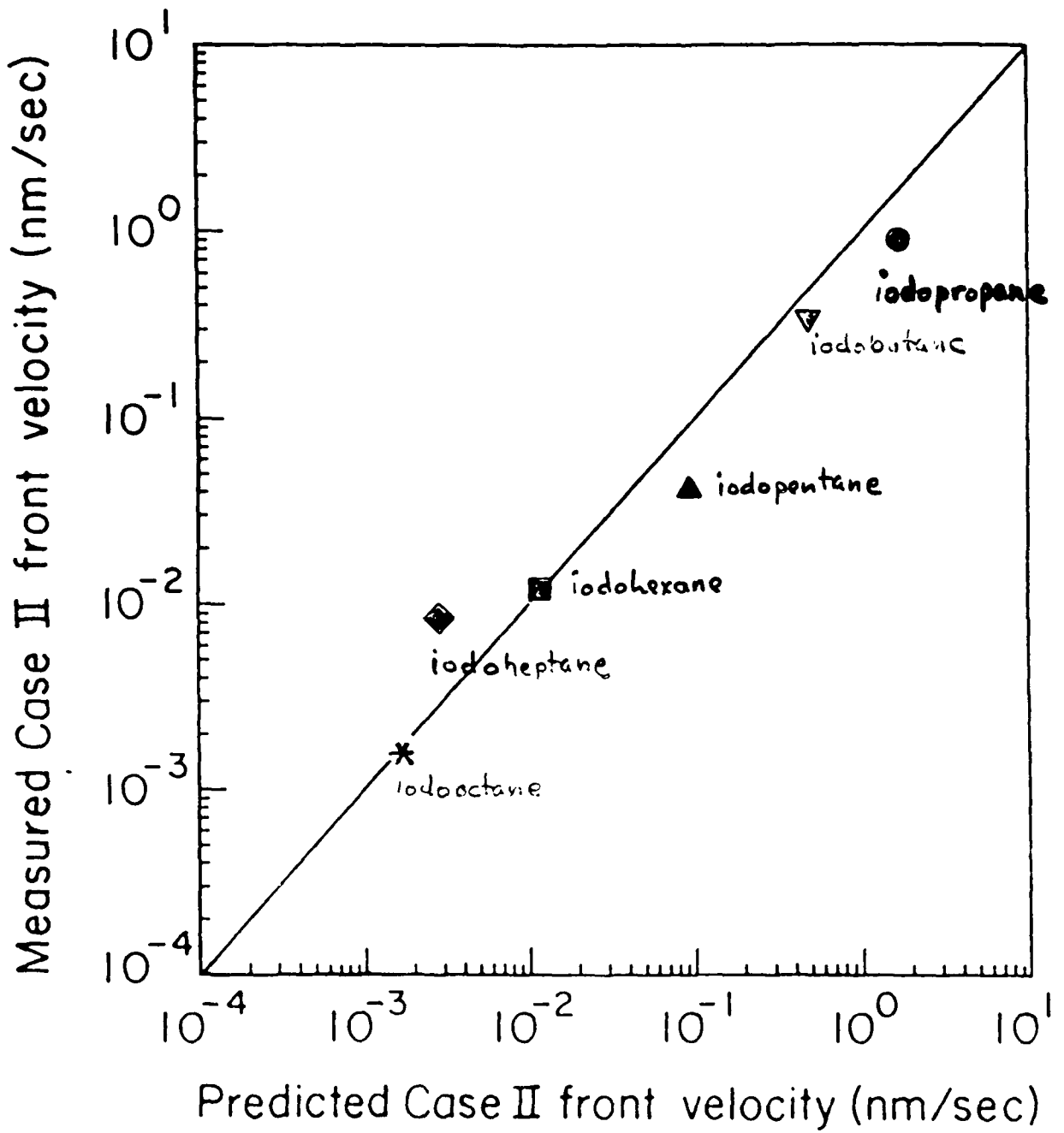


Figure 8

observed  $d\phi/dt$  at  $\phi_c$  increased markedly with  $P_{os}$  approximately as  $P_{os}^{1.2}$  as shown in Figure 9, in marked contradiction to the linear viscous model. One of the initial puzzles in our results on polystyrene exposed to the entire series of the iodoalkanes at constant vapor activity was the very strong increase in the swelling rate at  $\phi_c$  as the size of the iodoalkane molecule (or  $n$ ) was decreased [3]. However for solvent molecules with the same activity but different molecular volumes  $\Omega$ , the osmotic pressure  $P_{os}$  is inversely proportional to  $\Omega$  as can be seen from Eq. 2. When the observed  $d\phi/dt$  at  $\phi_c$  for the various iodoalkanes at constant activity is plotted versus the calculated osmotic pressure  $P_{os}$  as shown in Figure 9 these data are in excellent agreement with Lasky's where the  $P_{os}$  was changed for iodohexane simply by changing the vapor activity .

The strong dependence of  $d\phi/dt$  at  $\phi_c$  on  $P_{os}$ , which is similar to the strong dependence of strain rate on yield stress for glassy polymers, as well as the nearly discontinuous increase in  $D$  at  $\phi_c$ , leads us to propose that Case II diffusion should be interpreted as a physico-chemically driven (osmotic pressure) yielding of the glassy polymer. Rather than a slow creep phenomenon reaching a critical state when the polymer is plasticized so that  $T_g$  falls below the experimental temperature, the polymer reaches a critical state when the osmotic pressure exceeds the yield stress versus concentration envelope. That this is a reasonable hypothesis can be seen on Figure 10 where we plot both the yield stress in compression as a function of solvent volume fraction  $\phi$  (after Kambour) and the osmotic pressure as a function of  $\phi$  for several different iodoalkanes.

This hypothesis suggests that Case II diffusion can occur for polymers with  $T_g$ 's too high to be plasticized to a rubbery state if the

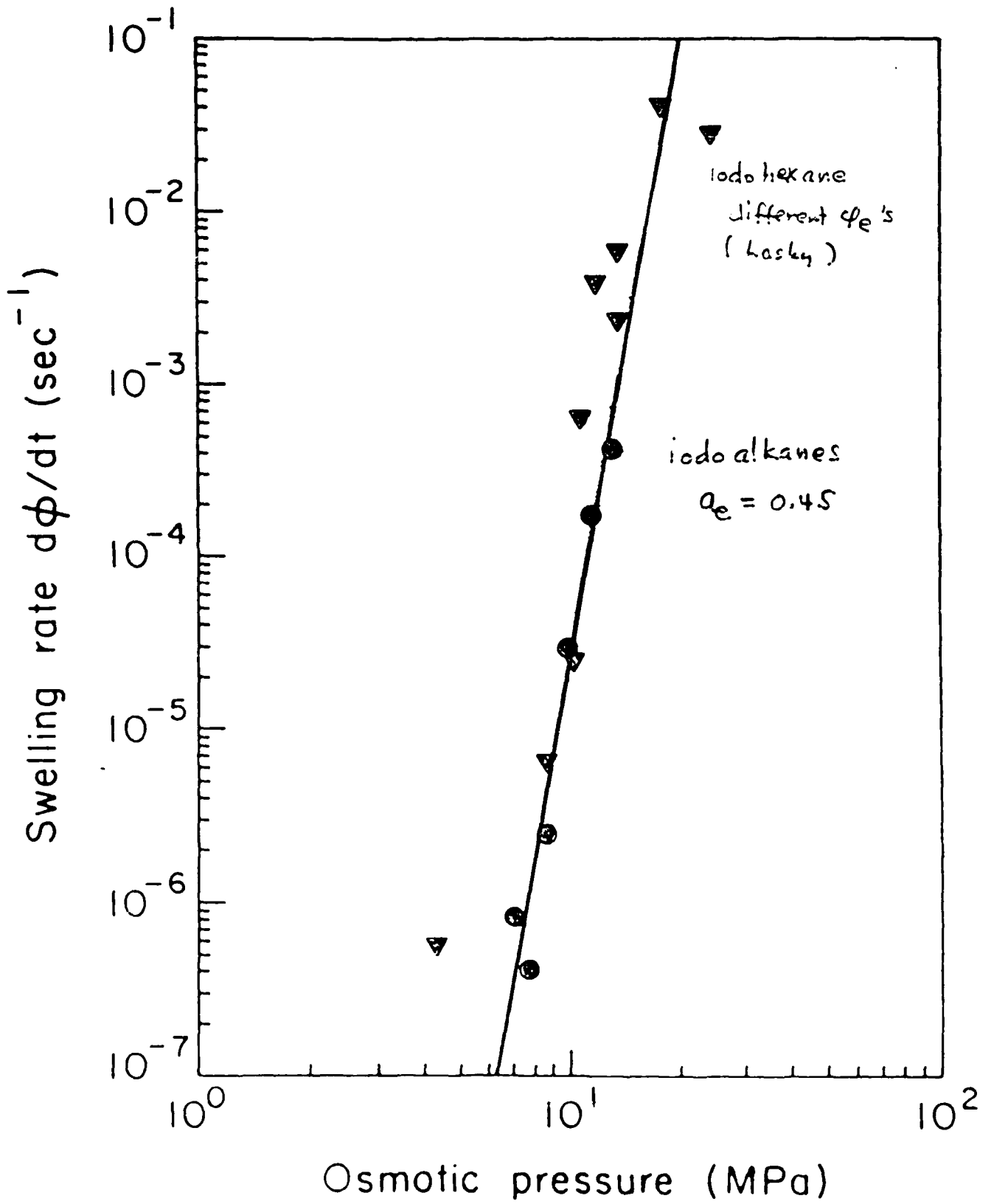


Figure 9

$$P_{os} = \frac{k_B T}{\Omega} \ln \frac{a_e}{a}$$

partial molecular volume

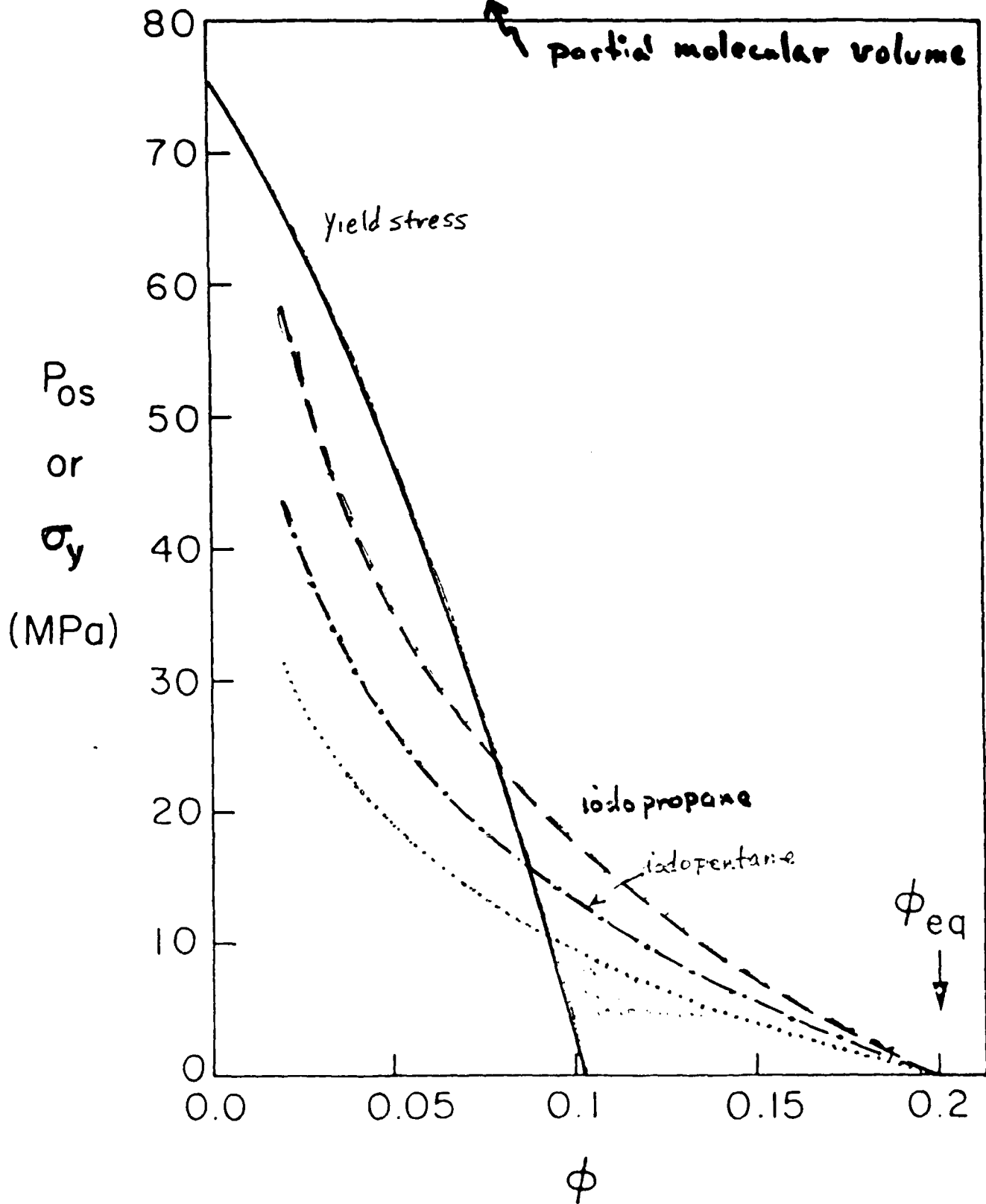
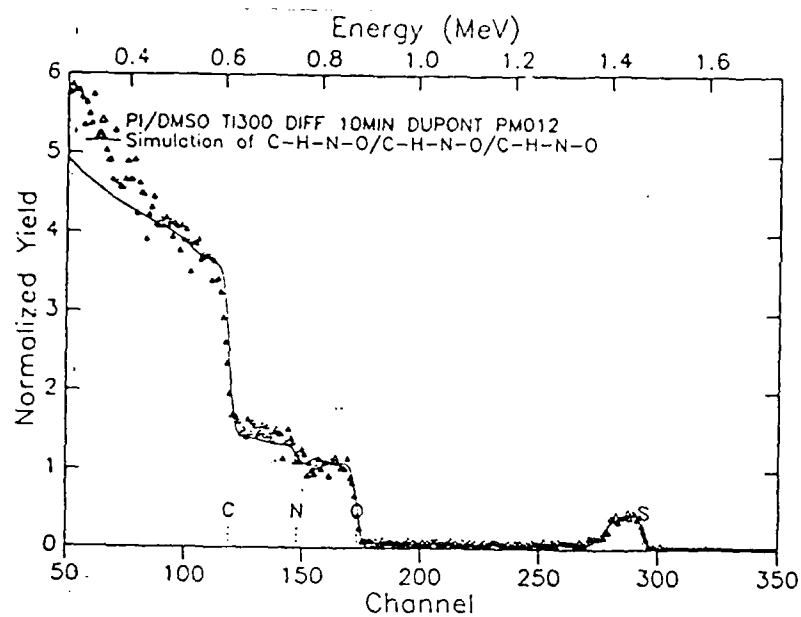


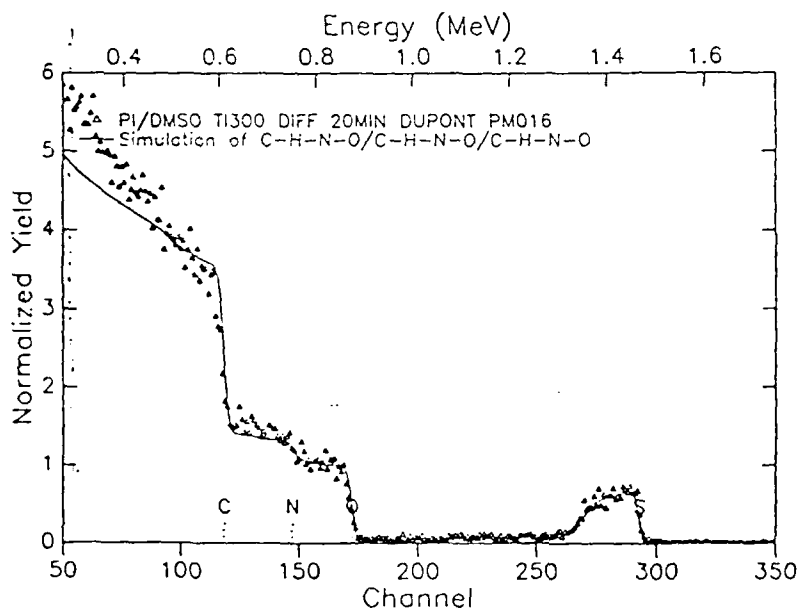
Figure 10

osmotic pressure is high enough and the yield stress low enough, a prediction which has recently been confirmed for the polyimides. Figure 11 shows three RBS spectra taken from a PMDA-ODA polyimide exposed to dimethylsulfoxide (DMSO) for 10, 20 and 40 minutes, respectively. A front forms and moves at roughly constant velocity into the polymer and the gradient in DMSO concentration behind the front is much lower than that ahead of the front (although significantly, it is not zero in this case). DMSO diffuses into the polyimide by Case II diffusion. Yet mechanical testing of the swollen polyimide at room temperature reveals that it is definitely glassy as would be expected since its glass transition temperature is well above 400°C so that even relatively large volume fractions of solvent are unlikely to plasticize it enough so that its  $T_g$  is below room temperature. Moreover we find that treatments of the polyimide which lower its yield stress (or increase its strain rate at constant stress) in a direction normal to the film surface (uniaxial or biaxial orientation in the film plane, for instance) also increase the velocity of the Case II front. This evidence, taken together with the exceptionally strong dependence of the swelling rate on osmotic pressure for PS, suggests that Case II diffusion is really a chemically driven yielding of the polymer glass.

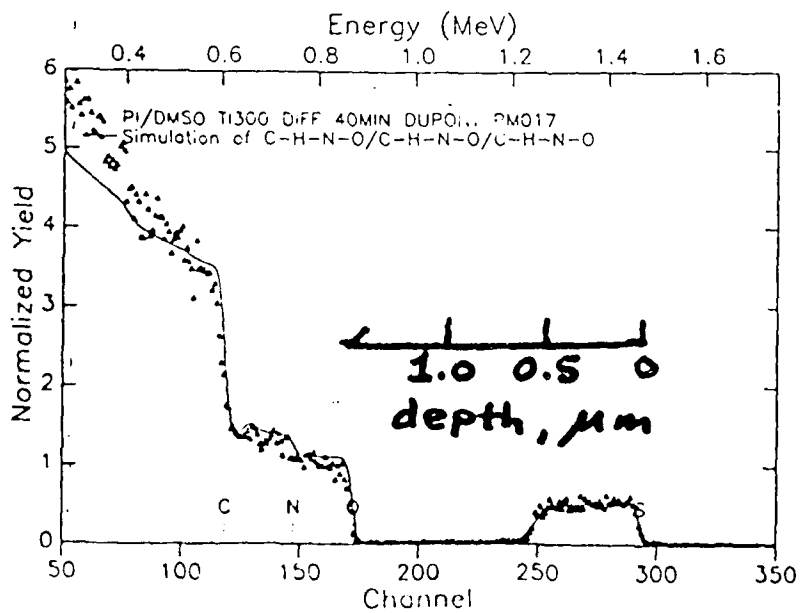
# DMSO diffuses into polyimide by Case II diffusion



DMSO exposure  
10 min



DMSO exposure  
20 min



DMSO exposure  
40 min

Figure 11

## References

1. "Ion Beam Analysis of Solvent Diffusion in Polystyrene", T. P. Gall, PhD Thesis, Cornell University, 1989.
2. "The Study of Polystyrene Surface Swelling by Quartz Crystal Microbalance and Rutherford Backscattering Techniques", R. Ognjanovic, C.-Y. Hui and E. J. Kramer, MSC Report #6551, J. Mat. Sci., in press.
3. "Case II Diffusion: Effect of Solvent Molecule Size", T. P. Gall, R. C. Lasky and E. J. Kramer, MSC Report #6706, submitted for publication to Polymer.
4. "Rutherford Backscattering Analysis of Case II Diffusion in Polystyrene", R. C. Lasky, PhD Thesis, Cornell University, 1986.
5. "Chemically-Driven Deformation of Polymers", C.-Y. Hui, K.-C. Wu, R.C. Lasky and E.J. Kramer, (MSC Report #5851) Trans ASME, J. of Electronic Packaging, **111** 68-73 (1989).
6. "Case II Diffusion in Polymers I: Transient Swelling", C.-Y. Hui, K.-C. Wu, R.C. Lasky and E.J. Kramer, (MSC Report # 5826) J. Appl. Phys., **61** 5129-5136 (1987).
7. "The Initial Stages of Case II Diffusion at Low Penetrant Activities", R.C. Lasky, E.J. Kramer and C.-Y. Hui, (MSC Report #6148), Polymer, **29** 673 (1988).
8. "Case II Diffusion in Polymers II: Steady State Front Motion", C.-Y. Hui, K.-C. Wu, R.C. Lasky and E.J. Kramer, (MSC Report #5844) J. Appl. Phys., **61** 5137-5149 (1987).
9. "The Temperature Dependence of Case II Diffusion", R.C. Lasky, E.J. Kramer and C.-Y. Hui, (MSC Report #6184), Polymer, **29** 1131 (1988).
10. "The Diffusion of Deuterated Toluene in Polystyrene", T. P. Gall and E. J. Kramer, submitted for publication.